



# First insights into the role of wall shear stress in the development of a distal stent graft induced new entry through computational fluid dynamics simulations

Anja Osswald<sup>1^</sup>, Alexander Weymann<sup>1</sup>, Konstantinos Tsagakis<sup>1</sup>, Alina Zubarevich<sup>1</sup>, Matthias Thielmann<sup>1</sup>, Bastian Schmack<sup>1</sup>, Arjang Ruhparwar<sup>1</sup>, Christof Karmonik<sup>2</sup>

<sup>1</sup>Department of Thoracic and Cardiovascular Surgery, West-German Heart and Vascular Center Essen, Essen, Germany; <sup>2</sup>Translational Imaging Center, Houston Methodist Research Institute, Houston, TX, USA

**Contributions:** (I) Conception and design: A Osswald, A Weymann, C Karmonik; (II) Administrative support: A Weymann, A Ruhparwar; (III) Provision of study materials or patients: K Tsagakis, A Osswald; (IV) Collection and assembly of data: A Osswald; (V) Data analysis and interpretation: A Osswald, C Karmonik; (VI) Manuscript writing: All authors; (VII) Final approval of manuscript: All authors.

**Correspondence to:** Anja Osswald, MD. Department of Thoracic and Cardiovascular Surgery, West-German Heart and Vascular Center Essen, Hufelandstraße 55, 45147 Essen, Germany. Email: Anja.osswald@uk-essen.de.

**Background:** Distal stent graft induced new entry (dSINE) is an emerging complication after frozen elephant trunk (FET) procedure. The aim of this computational fluid dynamics (CFD) study was to investigate the role of wall shear stress (WSS) after the development of dSINE based on hemodynamic changes.

**Methods:** Aortic diameter and WSS of five patients who developed a dSINE after FET procedure were retrospectively analyzed before and after the occurrence of dSINE. Patient-specific 3-dimensional surface models of the aortic lumen were reconstructed from computed tomography angiographic datasets (pre dSINE: n=5, dSINE: n=5) to perform steady-state CFD simulations with laminar blood flow and zero pressure outlet conditions. WSS was calculated at the level of the stent graft (SG), the landing zone of the SG and at a location further distal to the SG, as well as on the outer and inner curvature of the aorta from SG center to its distal end.

**Results:** Post dSINE occurrence, median WSS increased significantly from 0.87 [interquartile range (IQR): 0.83–1.03] to 1.55 (IQR: 1.09–2.70) Pa, (P=0.043) within the SG and from 1.22 (IQR: 0.81–1.44) to 1.76 (IQR: 1.55–3.60) Pa, (P=0.043) at the landing zone of the SG. A non-significant increase from 1.22 (IQR: 0.59–3.50) to 2.58 (IQR: 1.16–3.78) Pa, (P=0.686) further downstream was observed. WSS at the outer curvature of the SG was significantly higher compared to WSS at the inner curvature for dSINE.

**Conclusions:** Adverse hemodynamic conditions in the form of elevated WSS consist inside and at the distal end of the SG as well as at the outer curvature of the aorta, which may contribute to weakening of the aortic wall. These new findings emphasize the relevance and potential of WSS in dSINE for additional adverse events, such as aortic rupture. Further prospective studies are warranted to explore if the combination of clinical parameters with WSS might be useful to decide which patients require an urgent reintervention in terms of a SG extension.

**Keywords:** Wall shear stress (WSS); computational fluid dynamics simulation; distal stent graft induced new entry (dSINE); frozen elephant trunk (FET); aortic dissection

Submitted Sep 02, 2022. Accepted for publication Nov 25, 2022. Published online Feb 13, 2023.

doi: 10.21037/jtd-22-1206

**View this article at:** <https://dx.doi.org/10.21037/jtd-22-1206>

<sup>^</sup> ORCID: 0000-0002-2315-880X.

## Introduction

The frozen elephant trunk (FET) operation is a hybrid procedure that allows the replacement of the aortic arch with a surgical prosthesis and the treatment of an aortic dissection of the descending aorta with a stent graft (SG). The FET is a save option for treating complex aortic pathologies (1). Nevertheless, there are complications to be considered, like the newly described pathology of a distal stent graft induced new entry (dSINE), defined as a new aortic entry tear caused by the SG itself (2). It describes the rupture of the inner aortic wall at the free edge of the distal SG end, which corresponds to a covered rupture of the aortic wall in the sense of a perforated aortic ulcer. This lesion may be perfused by blood or thrombose. dSINE represents a risk factor for aortic rupture and is considered an indication for further endovascular or open surgical treatment (3).

A recent literature review and an analysis from the European Registry of Endovascular Aortic Repair Complications reported incidences of dSINE after thoracic endovascular aortic repair (TEVAR) of 7.9% and 4.8%, respectively (4,5). Incidence after FET varies from 6–13% (5,6).

Computational fluid dynamics (CFD) analysis is a method to calculate blood flow by solving the governing equations of fluid mechanics and so allow for the quantitative assessment of hemodynamics by simulating blood flow dynamics and its interaction with the arterial wall (7). While medical imaging provides the anatomical and physiological details, CFD simulation allow for visualization of velocity flow fields, pressure distribution,

wall shear stress (WSS) and oscillating shear index. CFD simulations are being successfully applied in the field of aortic pathologies and have improved the understanding of the development and progression of these complications. CFD simulations can be performed by either using computer-generated or from computed tomography angiography (CTA) or magnetic resonance imaging (MRI) images reconstructed, patient-specific 3-dimensional (3D) models. CFD simulations have been used to analyze blood flow in diseased aortas, such as flow patterns in aortic aneurysms, aortic dissections, and changes before and after endovascular repairs (8-13). In particular, WSS, the tangential force to the arterial wall generated from the blood flow, has been of special interest, as the endothelial cells have been shown to sense the shear forces created by the blood flow and react adversely if the flow decreases or becomes irregular (14-17). Due to the limitations of *in-vivo* measurements, CFD simulations provide an excellent option for WSS assessment. The parameters obtained in CFD, can be incorporated into clinical application, either in disease assessment or treatment planning.

According to current studies, both the incidence and the risk factors for the development of dSINE in patients after FET surgery remain unclear. While mostly mechanic factors are indicated, our hypothesis was that also adverse hemodynamic conditions may be a contributing factor to some extent. Therefore, the motivation for our study was to investigate the role of WSS, a hemodynamic parameter sensed directly by the endothelial cells, in dSINE development using CFD. More specifically, streamlines and local distributions of the WSS prior and after the development of dSINE were evaluated at the landing zone as well as the surrounding area. We present the following article in accordance with the STROBE reporting checklist (available at <https://jtd.amegroups.com/article/view/10.21037/jtd-22-1206/rc>).

## Methods

### Study design

The study was conducted in accordance with the Declaration of Helsinki (as revised in 2013). The study was approved by institutional ethics board of the University Duisburg-Essen (No. 22-10561-BO) and individual consent for this retrospective analysis was waived. It is based on CTA examinations of patients who received a FET surgery and developed dSINE during follow up {median follow-

### Highlight box

#### Key findings

- WSS increased within the SG and at its distal landing zone after the development of a dSINE.

#### What is known and what is new?

- Suggested risk factors for dSINE after frozen elephant trunk are either associated with the SG itself or aortic characteristics. Hemodynamic parameters assessed by computational fluid dynamics simulations, such as WSS might also play an important role in dSINE and for additional adverse events such as aortic rupture.

#### What is the implication, and what should change now?

- Elevated WSS after dSINE may be a risk factor for further complications. A close follow up in patients with dSINE is crucial.

up of 9.5 years [interquartile range (IQR): 9.4–10.9]]. Between 2013 and 2018, 5 patients developed a dSINE after initial FET operation. From those patients, CTAs were obtained prior (pre dSINE group) and after (dSINE group) the development of dSINE and CFD simulations were performed for each case.

### *Patient characteristics*

Patients were treated for either acute or chronic aortic dissections. Detailed report of our surgical technique and management for the FET procedure had been previously described (18). In brief, FET procedure was performed via median sternotomy using cardiopulmonary bypass and circulatory arrest in mild hypothermia (target temperature 22 °C). Cannulation of the right subclavian artery was favored and used for continuous cerebral perfusion during the arch repair. Cerebrospinal fluid drainage was routinely used in all elective cases. The aortic arch was replaced using an E-vita Open plus prosthesis (Jotec® Inc., Hechingen, Germany) which was introduced downstream in guide-wire technique. The size of the SG was chosen according to true lumen (TL) diameter with the aim to avoid oversizing over 10%. After deployment of the SG, the FET fixation was performed circumferentially to the aorta. The proximal end was either sutured to the native aorta or to the prosthesis of the ascending aorta and reimplantation of the supraaortic vessels was performed during rewarming.

Four of the five dSINE patients underwent elective endovascular treatment using distal SG extension. As TEVAR was performed as second-stage procedure sizing referred to the proximal landing zone with aiming for a maximum of 10% oversizing and an intended device overlap of 3–5 cm. Median TEVAR length was 160 cm (IQR: 150–164), using either Bolton Relay or in one case Evita thoracic 3G Straight-Cut. Primary success rate of the reinterventions was 100%. One patient decided against the recommended TEVAR treatment.

### *CTA image data preprocessing*

Postoperative CTA scans of the chest and abdomen were obtained according to the standardized electrocardiogram (ECG)-gated breathhold aortic protocol. Only scans of clinically diagnostic quality and without motion artifacts were included. These scans yielded consecutive axial slices with slice thickness ranging from 1 to 1.5 mm covering the entire aorta, which were adequate to segment the

aortic lumen in all cases. According to guidelines, follow-up contrast-enhanced CTAs of the entire aorta using a similar imaging protocol were acquired after 3–6 months and annually thereafter (19). CTA was either performed using a dual source 128-slice CT scanner (SOMATOM Definition Flash; Siemens Healthineers, Forchheim, Germany) or already conducted at the referring outside facility. dSINE was defined as a new tear caused by the SG of the FET prosthesis, excluding tears created by natural disease progression (2). Patient-specific dissection geometries were reconstructed from the CTA images after FET implantation. Geometric models were created from the last CTA before the development of dSINE (pre dSINE group) as well as from the CTA images, where dSINE was first detected (dSINE group).

Due to the complexity of the aortic disease, a semi-manual technique was employed to obtain a 3D surface model of the aortic lumen as reported previously (8). In short, first, for each CTA image, a 2D mask was created by manually identifying the lumen. These masks were combined and stored as a stereolithographic file representing a 2D triangulated surface mesh of the lumen. Imported into a 3D modelling software (Meshmixer, version 3.5.474), the region of interest comprising the ascending aorta, the aortic arch including the supra-aortic vessels, the descending aorta and the iliac arteries was isolated and the corresponding surface was smoothed by adaptive remeshing.

Aortic measurements were performed for each group in Horos® (Nimble Co LLC d/b/a Purview in Annapolis, MD, USA; 4 Version 3.3) using double oblique 3D multiplanar reconstruction. The changes of the aortic diameter and TL diameters (mm) were assessed at the level of the stented segment (L1), at the landing zone of the SG (L2) and 2 cm further distally to the SG ending (L3) (Figure 1A). All diameters were measured perpendicular to the centerline.

### *CFD simulations*

The smoothed 2D meshes were imported into Star CCM+ (Siemens cd-adapco, 2020.3, version 15.06.007-R8), to create polyhedral meshes, with a median mesh size of 509,269 (IQR: 126,501–1,927,197). Mesh independence of these kinds of simulations were previously investigated and assured (19).

The blood flow simulations were performed by solving the Navier-Stokes equations and were based on the finite volume method. Walls were assumed to be rigid. Simulation settings included laminar flow (Reynolds numbers in the aorta are in the order of 2,000) and the blood was modeled

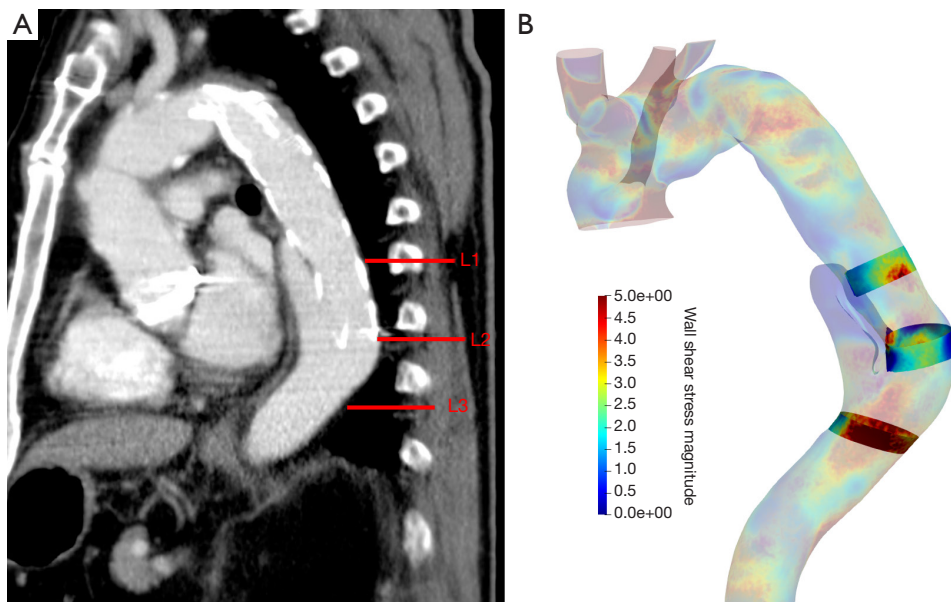


**Figure 1** Aortic and TL diameters were measured at the level of the stented segment (L1), at the landing zone (L2) and 2 cm further distally to the SG ending (L3) (A). WSS was assessed at the same locations (B). TL, true lumen; SG, stent graft; WSS, wall shear stress.

as a Newtonian fluid with a dynamic viscosity of  $0.004 \text{ Pa}\cdot\text{s}$  and a constant density of  $1,050 \text{ kg/m}^3$ . Blood is an inhomogeneous fluid, but the effect of non-Newtonian behaviour in large vessels is negligible. Therefore, modeling the blood as a Newtonian fluid a satisfactory assumption for the aorta. Due to the retrospective design of the study, direct flow or pressure measurements of inflow conditions were not available. Therefore, inflow was set at a constant cardiac output velocity of  $0.4 \text{ m/s}$  approximating the average normal flow velocity in the ascending aorta (8), outlet boundaries were defined as zero pressure outlets (i.e., no distally increased vascular resistance). Extensions were created at the ascending aorta and all vessel branches, to have a fully developed flow at the inlet and to avoid outlet boundary conditions effects on the outlets.

### Data analysis

Streamlines were used to visualize blood flow to gain a first understanding of the flow patterns and their changes introduced by dSINE occurrence. WSS was then calculated as a quantitative measure. Both procedures were performed within Paraview (Kitware Inc., version 5.9.0). WSS values were extracted at the previously defined regions of interest L1–L3 defined from the clinical CT images. L2 was first chosen to be at the location of the distal SG end, and then L1 and L3 placed 2 cm proximal and

distal to L3. In this way, all locations where WSS measurements were taken were uniquely defined by SG end. The actual area of measurement was the same for all cases and was technically realized by using the box clipping tool available in the Paraview software (Figure 1B). For each location, the WSS magnitude was determined by calculating the mean value of the so isolated aortic area. The WSS magnitude was also measured on both the inner and outer curvature of the aorta, from the center of the SG to its distal end.

### Statistical analysis

Statistical analysis was performed using SPSS (version 27, SPSS, Chicago, IL, USA). All results are presented as median and IQR. Statistical analyses of the evaluated parameters were performed using the non-parametric Wilcoxon signed-rank test and a P value  $<0.05$  was defined as statistically significant.

## Results

### Patient data

Median age at the initial FET operation was 55 years (IQR: 54–65 years). Three patients were treated for chronic, two for acute aortic dissection. All patients demographics and FET characteristics are displayed in Table 1. dSINE was diagnosed in routine follow-up and occurred after a median of

**Table 1** Patients and FET baseline characteristics after FET implantation

Patient demographics	Patients				
	#1	#2	#3	#4	#5
Age (years)	44	55	73	65	54
Male/female	Male	Male	Male	Female	Male
DeBaKey classification	1	3	3	1	1
False lumen extension	Yes	Yes	Yes	No	Yes
Thoracic	Yes	No	Yes	–	Yes
Abdominal	Yes	Yes	Yes		
True lumen collapse	No	Yes	No	No	No
Underlying disease	CAD	CAD	CAD	AAD	AAD
Connective tissue disorder	No	No	No	No	No
Coronary artery disease	No	No	No	Yes	No
Previous sternotomy	Yes	No	Yes	No	Yes
Previous aortic surgery	Yes	No	Yes	No	Yes
FET characteristics					
SG anastomosis zone	3	1	2	3	2
SG diameter, mm	24	28	28	28	28
SG length, mm	150	130	130	130	130
SG distal landing zone	Th 8-9	Th 5	Th 8-9	Th 8-9	Th 8-9

FET, frozen elephant trunk; CAD, chronic aortic dissection; AAD, acute aortic dissection; SG, stent graft.

2.75 years (IQR: 2.03–6.87 years) after initial FET operation.

### Streamlines

In all patients, streamline visualization demonstrated low blood flow and non-laminar vortices apparent within the SG (*Figure 2*). A certain volume of flow entered the false lumen (FL) of patient number (No.) 1, 3 and 5 through the entry tear. Flow in the FL was more complicated than in the TL, with the presence of separated, recirculating, disturbed, and turbulent flow. Blood flow within the FL of the dSINE varied among these patients. In patient No. 1 and 2 characteristics of flow pattern were similar to FL flow. In patient No. 3–5 no streamlines were apparent within the dSINE.

### WSS

Significantly elevated WSS magnitudes were observed within the SG and at the landing zone of the SG after the

development of dSINE (*Figure 3*).

Median WSS within the SG increased from 0.87 Pa (IQR: 0.83–1.03 Pa) in the pre dSINE group to 1.55 Pa (IQR: 1.09–2.70 Pa) in the dSINE group ( $z = -2.023$ ,  $P = 0.043$ ). At the landing zone of the SG, WSS increased from 1.22 Pa (IQR: 0.81–1.44 Pa) to 1.76 Pa (IQR: 1.55–3.60 Pa) ( $z = -2.023$ ,  $P = 0.043$ ) after the development of dSINE. Distally to the SG there was no statistically significant difference between the pre dSINE [1.22 Pa (IQR: 0.59–3.50 Pa)] and the dSINE group but WSS was still elevated in the latter [2.58 Pa (IQR: 1.16–3.78 Pa)] ( $z = -0.405$ ,  $P = 0.686$ ).

WSS at the outer curvature of the SG was significantly higher as compared to the inner curvature after dSINE occurrence. Prior to the dSINE, median WSS at the mid-level to the end of the SG was 0.71 Pa (IQR: 0.28–0.95 Pa) at the inner curvature and 1.33 Pa (IQR: 0.63–1.61 Pa) at the outer curvature ( $z = -1.567$ ,  $P = 0.117$ ). After the occurrence of dSINE median WSS at the outer curvature was 1.96 Pa (IQR: 1.58–3.62 Pa) and 1.18 Pa (IQR: 1.91–1.56 Pa)

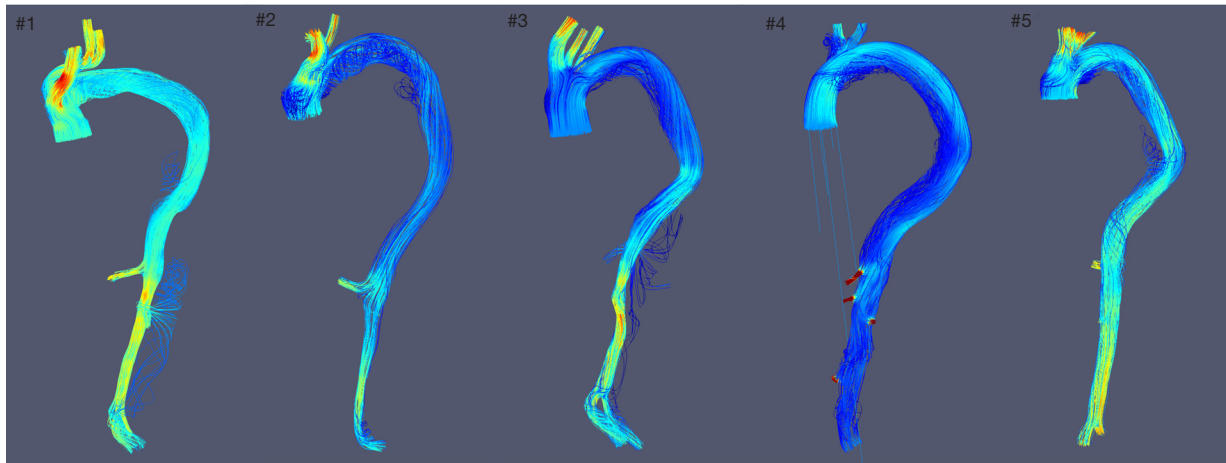


**Figure 2** Streamlines visualize the blood flow patterns in the aorta. Streamlines were colored by the magnitude of the fluid velocity. Red represents high flow, blue represents low flow velocity.

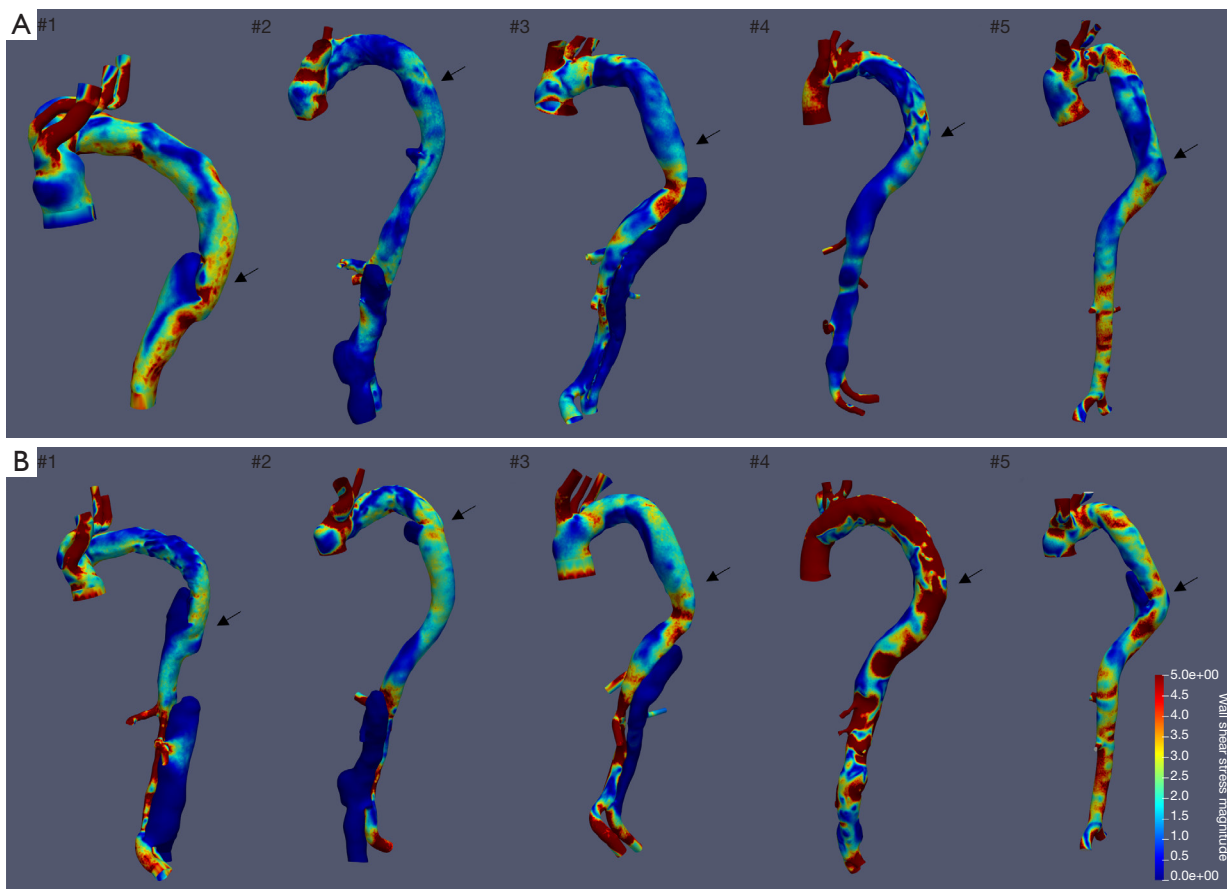


**Figure 3** WSS is presented for each patient prior (A) and after the development of dSINE (B) (arrows show the distal end of the FET). WSS was significantly elevated after the development of dSINE (B) within the SG and at its distal end. In patient No. 1, 3 and 5 a localized WSS increase was apparent at the landing zone of the SG and/or distally (A). In patient No. 4 WSS post-dSINE was increased in the whole aorta. The streamlines, in *Figure 2* show, that flow with elevated velocity passes close to the anterior wall, thereby causing the higher WSS at that wall. WSS, wall shear stress; dSINE, distal stent graft induced new entry; FET, frozen elephant trunk; SG, stent graft.

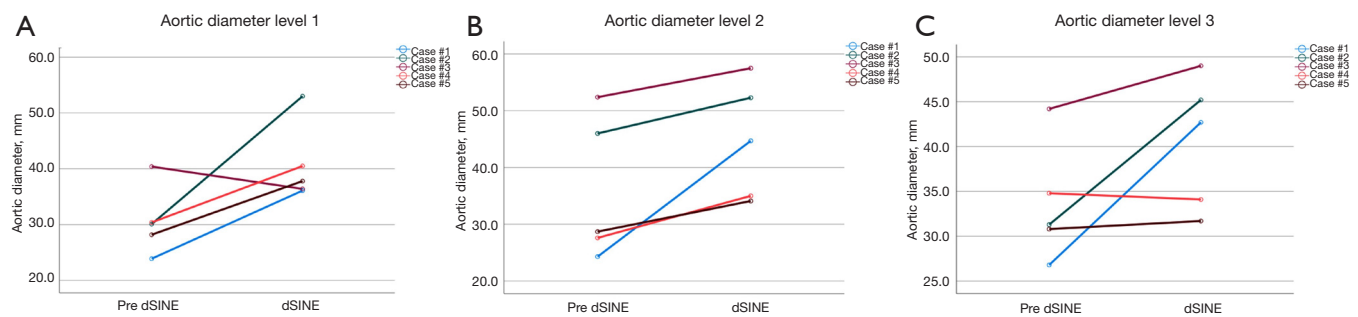


**Figure 4** Maximal aortic diameters of each patient are presented at the level of the stented segment (L1) (A), at the distal end of the SG (L2) (B) and 2 cm further distally to the SG ending (L3) (C). Median aortic diameter increased at all locations, reaching statistical significance at L2. dSINE, distal stent graft induced new entry; SG, stent graft.

( $z = -2.193$ ,  $P = 0.032$ ) at the inner curvature.

### Aortic characteristics

#### L1—segment at the SG level

Median total aortic diameter prior to dSINE was maximal 30.1 mm (IQR: 2.60–3.54 mm) and minimal 26.7 mm (IQR: 2.42–3.07 mm) and increased to 37.8 mm (IQR: 3.62–4.67 mm) and 33.4 mm (IQR: 32.8–4.24 mm), respectively, after the development of dSINE (no statistical significance) (Figure 4A). TL diameter (SG expansion) remained stable [pre dSINE: 28.7 mm (IQR: 26.0–30.1 mm) × 26.7 mm (IQR: 24.2–27.6) vs. dSINE: 28.6 mm (IQR: 25.2–29.6 mm) × 25.9 mm (IQR: 22.6–26.8 mm)].

#### L2—segment at landing zone of the SG

At the distal end of the SG median aortic diameter pre dSINE was 28.7 mm (IQR: 2.59–4.92 mm) maximal and 25.8 mm (IQR: 23.9–41.5 mm) minimal. For dSINE, the aortic diameter increased to 44.7 mm (IQR: 34.5–5.49 mm) × 43.4 mm (IQR: 3.15–46.0 mm), ( $z = -2.023$ ,  $P = 0.043$ ), (Figure 4B). The TL diameters remained stable [maximal diameters pre dSINE: 27.6 mm (IQR: 23.9–28.7 mm) vs. dSINE: 28.0 mm (IQR: 24.2–28.9 mm) ( $z = -1.084$ ,  $P = 0.279$ )].

#### L3—segment distally to the SG

Median aortic diameter was 31.3 mm (IQR: 28.8–39.5 mm) × 27.7 mm (IQR: 26.3–36.5 mm) pre dSINE and increased to 42.7 mm (IQR: 32.9–47.1 mm) × 32.5 mm (IQR: 29.3–44.6 mm) for dSINE ( $z = -1.753$ ,  $P = 0.08$ ;  $z = -0.135$ ,  $P = 0.893$ , respectively), (Figure 4C). Similarly to L1 and L2, the TL lumen diameter remained stable [maximal diameters pre dSINE: 31.3 mm (IQR: 28.8–33.9 mm) vs. dSINE: 31.7

mm (IQR: 29.3–44.6 mm)].

FL thrombosis was achieved at the level of the SG in patient No. 1, 2, 3 and 5 after the initial FET operation. In three patients (No. 1–3), the FL distally to the SG landing zone, at the thoracoabdominal aorta remained patent. Patient No. 4 had an isolated arch pathology, therefore no FL was present at the thoracic and abdominal level.

### Discussion

dSINE is a complication occurring not infrequently with incidences of 4.8–7.9% after TEVAR and up to 13% after FET (20). Several risk factors for SG-associated complications have been reported including aortic wall fragility, natural progression of the aortic disease and elastic recoil (21,22). After TEVAR, excessive oversizing ratio, less taper ratio, larger aortic diameter, increased length of the SG and enlarged angle between the SG and the TL have been reported as risk factors for dSINE (23–25). The occurrence of dSINE may result in a patent FL with subsequent aneurysmal expansion and the risk of rupture (26). Given the severity of these complications, it is desirable to understand and predict the progression of this disease.

This study focused on functional parameters within the aorta in patients who developed a dSINE after FET. A comparison of WSS, streamlines and aortic characteristics was drawn before and after the development of dSINE. A significant increase of WSS after the development of the dSINE with minimal flow within the dSINE itself was found, as well as a significant aortic dilatation at the landing zone of the SG. The main focus of interest was at L2, at the transition zone between the SG and the aorta, as this is where the dSINE originates. WSS in the surrounding

area (L1, L3) was assessed to screen for alterations in WSS patterns, since abrupt changes in WSS may lead to increased mechanical stress on the aortic wall. WSS plays a key role as a regulator in vascular biology. Low WSS is known to contribute to arteriosclerotic formation (27). In contrast, high WSS contributes to atherosclerotic plaque destabilization, damages the endothelial surface of the aortic wall, leading to its weakening and potentially causes a rupture in the process (10). Studies showed that WSS elevation occurs at the entrance or at the narrowest part of the stenosed vessels as well as at the bifurcation and at the outer side of curved vessels and might either lead to rupture or aneurysm formation (28,29).

In our study, WSS increased significantly after the occurrence of dSINE within the SG and at its distal end. As the aortic wall at L1 is protected by the SG itself, the WSS increase should not be regarded as direct damage to the aortic wall, but as an indication that hemodynamics in the aorta change after the development of the dSINE. The SG itself is considered to present a pulsatile mechanical stimulus interacting with the aortic wall, which eventually may cause a new tear. This effect may be reflected by the here seen elevated WSS at the landing zone of the SG. Interestingly, while dSINE formed at the inner curvature of the aorta, significant WSS elevation occurred on the outer curvature. This effect was not seen to this same extent prior to dSINE. Several studies discussed the permanent exposure of the aortic wall to the forces of the SG, which may cause anatomical changes to the aorta, as a potential risk factor for dSINE (22,30). Accordingly, in our previous study, a greater dorso-lateral movement of the SG within the aorta was associated with the occurrence of dSINE after FET (31). The observed WSS elevation post dSINE may be secondary to the impact of the described force of the SG on the aorta and may be an indicator for the risk of rupture of the dSINE as it poses an adverse hemodynamic environment. It should also be noted, that we observed prior to dSINE formation, elevated WSS at this location, which may merit further investigation.

In addition, patient-specific aortic anatomy represents an important factor in the development of dSINE. Measurements of the aortic diameter revealed a stable TL diameter, but an increase in the total aortic diameter, and therefore the detected increase has to be attributed to the formation of the new FL of the dSINE at level L1–L2, and FL dilatation at L3 reaching statistical significance at the distal end of the SG (L2). Correspondingly, WSS was elevated at L2. Previous studies showed that WSS plays a

key role in FL dilatation (32). It should also be noted, that we observed prior to dSINE formation, elevated WSS at this location, which may merit further investigation.

### **Limitations**

The present study was limited by its retrospective nature and the small number of patients due to the incidence rate of this complication. The limitations of our CFD simulations are similar to these kinds of simulations and are related to the assumptions made in the creation of the fluid model such as laminar blood flow, constant inflow velocity and rigid walls. In case of a completely thrombosed FL, CFD simulations only included the patent TL.

Due to study design, WSS measurements were only available as averages over the entire cardiac cycle. Consequently, reported WSS differences prior and post dSINE should be interpreted accordingly. To minimize potential selection bias the regions of interest were defined prior to visualization of WSS.

### **Conclusions**

In this study, WSS increased significantly after the occurrence of dSINE within the SG and at its landing zone. WSS was also elevated at the outer compared to the inner curvature of the aorta. Those results provide insight in the hemodynamics and underline the relevance and peril of this complication, since elevated WSS may lead to weakening of the aortic wall may be a risk factor for the progression or development of new dissections sites. We feel in the light of our findings, that hemodynamics parameters assessed by CFD simulations can be of special value in cases, when clinical parameter do not offer a definitive answer. The combination of clinical parameters with WSS might be useful to decide which patients require an urgent reintervention in terms of a SG extension. Our results encourage further studies with larger patient numbers to make such a recommendation.

### **Acknowledgments**

*Funding:* AO was supported as a Clinician Scientist within the University Medicine Essen Academy (UMEA) program, funded by the German Research Foundation (DFG) and the Faculty of Medicine, University of Duisburg-Essen (Grant No. FU 356/12-1).

## Footnote

*Reporting Checklist:* The authors have completed the STROBE reporting checklist. Available at <https://jtd.amegroups.com/article/view/10.21037/jtd-22-1206/rc>

*Data Sharing Statement:* Available at <https://jtd.amegroups.com/article/view/10.21037/jtd-22-1206/dss>

*Conflicts of Interest:* All authors have completed the ICMJE uniform disclosure form (available at <https://jtd.amegroups.com/article/view/10.21037/jtd-22-1206/coif>). The authors have no conflicts of interest to declare.

*Ethics Statement:* The authors are accountable for all aspects of the work in ensuring that questions related to the accuracy or integrity of any part of the work are appropriately investigated and resolved. The study was conducted in accordance with the Declaration of Helsinki (as revised in 2013). The study was approved by institutional ethics board of the University Duisburg-Essen (No. 22-10561-BO) and individual consent for this retrospective analysis was waived.

*Open Access Statement:* This is an Open Access article distributed in accordance with the Creative Commons Attribution-NonCommercial-NoDerivs 4.0 International License (CC BY-NC-ND 4.0), which permits the non-commercial replication and distribution of the article with the strict proviso that no changes or edits are made and the original work is properly cited (including links to both the formal publication through the relevant DOI and the license). See: <https://creativecommons.org/licenses/by-nc-nd/4.0/>.

## References

1. Tsagakis K, Wendt D, Dimitriou AM, et al. The frozen elephant trunk treatment is the operation of choice for all kinds of arch disease. *J Cardiovasc Surg (Torino)* 2018;59:540-6.
2. Dong Z, Fu W, Wang Y, et al. Stent graft-induced new entry after endovascular repair for Stanford type B aortic dissection. *J Vasc Surg* 2010;52:1450-7.
3. Li Q, Ma WG, Zheng J, et al. Distal Stent Graft-Induced New Entry After TEVAR of Type B Aortic Dissection: Experience in 15 Years. *Ann Thorac Surg* 2019;107:718-24.
4. Canaud L, Gandet T, Sfeir J, et al. Risk factors for distal stent graft-induced new entry tear after endovascular repair of thoracic aortic dissection. *J Vasc Surg* 2019;69:1610-4.
5. Czerny M, Eggebrecht H, Rousseau H, et al. Distal Stent Graft-Induced New Entry After TEVAR or FET: Insights Into a New Disease From EuREC. *Ann Thorac Surg* 2020;110:1494-500.
6. Czerny M, Schmidli J, Adler S, et al. Current options and recommendations for the treatment of thoracic aortic pathologies involving the aortic arch: an expert consensus document of the European Association for Cardio-Thoracic surgery (EACTS) and the European Society for Vascular Surgery (ESVS). *Eur J Cardiothorac Surg* 2019;55:133-62.
7. Ong CW, Wee I, Syn N, et al. Computational Fluid Dynamics Modeling of Hemodynamic Parameters in the Human Diseased Aorta: A Systematic Review. *Ann Vasc Surg* 2020;63:336-81.
8. Takeda R, Sato F, Yokoyama H, et al. Investigations into the Potential of Using Open Source CFD to Analyze the Differences in Hemodynamic Parameters for Aortic Dissections (Healthy versus Stanford Type A and B). *Ann Vasc Surg* 2022;79:310-23.
9. Armour CH, Menichini C, Milinis K, et al. Location of Reentry Tears Affects False Lumen Thrombosis in Aortic Dissection Following TEVAR. *J Endovasc Ther* 2020;27:396-404.
10. Zhu Y, Mirsadraee S, Asimakopoulos G, et al. Association of hemodynamic factors and progressive aortic dilatation following type A aortic dissection surgical repair. *Sci Rep* 2021;11:11521.
11. Midulla M, Moreno R, Negre-Salvayre A, et al. Impact of Thoracic Endografting on the Hemodynamics of the Native Aorta: Pre- and Postoperative Assessments of Wall Shear Stress and Vorticity Using Computational Fluid Dynamics. *J Endovasc Ther* 2021;28:63-9.
12. Polanczyk A, Podyma M, Trebinski L, et al. A Novel Attempt to Standardize Results of CFD Simulations Basing on Spatial Configuration of Aortic Stent-Grafts. *PLoS One* 2016;11:e0153332.
13. Polanczyk A, Piechota-Polanczyk A, Stefańczyk L. A new approach for the pre-clinical optimization of a spatial configuration of bifurcated endovascular prosthesis placed in abdominal aortic aneurysms. *PLoS One* 2017;12:e0182717.
14. Osswald A, Karmonik C, Anderson JR, et al. Elevated Wall Shear Stress in Aortic Type B Dissection May Relate to Retrograde Aortic Type A Dissection: A Computational Fluid Dynamics Pilot Study. *Eur J Vasc Endovasc Surg*

- 2017;54:324-30.
15. Karmonik C, Partovi S, Loebe M, et al. Computational fluid dynamics in patients with continuous-flow left ventricular assist device support show hemodynamic alterations in the ascending aorta. *J Thorac Cardiovasc Surg* 2014;147:1326-33.e1.
  16. Urschel K, Tauchi M, Achenbach S, et al. Investigation of Wall Shear Stress in Cardiovascular Research and in Clinical Practice-From Bench to Bedside. *Int J Mol Sci* 2021;22:5635.
  17. Roux E, Bougaran P, Dufourcq P, et al. Fluid Shear Stress Sensing by the Endothelial Layer. *Front Physiol* 2020;11:861.
  18. Jakob H, Dohle D, Benedik J, et al. Long-term experience with the E-vita Open hybrid graft in complex thoracic aortic disease†. *Eur J Cardiothorac Surg* 2017;51:329-38.
  19. Oßwald A. Identifikation hämodynamischer Risikofaktoren für eine retrograde Aortendissektion Typ A nach Aortendissektion Typ B mit Hilfe der Computational Fluid Dynamics-Technologie. Heidelberg: Medizinischen Fakultät der Ruprecht-Karls-Universität Heidelberg, 2018.
  20. Kreibich M, Bünte D, Berger T, et al. Distal Stent Graft-Induced New Entries After the Frozen Elephant Trunk Procedure. *Ann Thorac Surg* 2020;110:1271-9.
  21. Jang H, Kim MD, Kim GM, et al. Risk factors for stent graft-induced new entry after thoracic endovascular aortic repair for Stanford type B aortic dissection. *J Vasc Surg* 2017;65:676-85.
  22. Jánosi RA, Tsagakis K, Bettin M, et al. Thoracic aortic aneurysm expansion due to late distal stent graft-induced new entry. *Catheter Cardiovasc Interv* 2015;85:E43-53.
  23. Huang CY, Weng SH, Weng CF, et al. Factors predictive of distal stent graft-induced new entry after hybrid arch elephant trunk repair with stainless steel-based device in aortic dissection. *J Thorac Cardiovasc Surg* 2013;146:623-30.
  24. Pantaleo A, Jafrancesco G, Buia F, et al. Distal Stent Graft-Induced New Entry: An Emerging Complication of Endovascular Treatment in Aortic Dissection. *Ann Thorac Surg* 2016;102:527-32.
  25. Lortz J, Leinburger F, Tsagakis K, et al. Distal Stent Graft Induced New Entry: Risk Factors in Acute and Chronic Type B Aortic Dissections. *Eur J Vasc Endovasc Surg* 2019;58:822-30.
  26. Hughes GC. Stent graft-induced new entry tear (SINE): Intentional and NOT. *J Thorac Cardiovasc Surg* 2019;157:101-6.e3.
  27. Kwak BR, Bäck M, Bochaton-Piallat ML, et al. Biomechanical factors in atherosclerosis: mechanisms and clinical implications. *Eur Heart J* 2014;35:3013-20, 3020a-3020d.
  28. Karmonik C, Diaz O, Klucznik R, et al. Quantitative comparison of hemodynamic parameters from steady and transient CFD simulations in cerebral aneurysms with focus on the aneurysm ostium. *J Neurointerv Surg* 2015;7:367-72.
  29. Petuchova A, Maknickas A. Computational analysis of aortic haemodynamics in the presence of ascending aortic aneurysm. *Technol Health Care* 2022;30:187-200.
  30. D'cruz RT, Syn N, Wee I, et al. Risk factors for distal stent graft-induced new entry in type B aortic dissections: Systematic review and meta-analysis. *J Vasc Surg* 2019;70:1682-93.e1.
  31. Osswald A, Schucht R, Schlosser T, et al. Changes of stent-graft orientation after frozen elephant trunk treatment in aortic dissection. *Eur J Cardiothorac Surg* 2021;61:142-9.
  32. Sun Z, Chaichana T. A systematic review of computational fluid dynamics in type B aortic dissection. *Int J Cardiol* 2016;210:28-31.

**Cite this article as:** Osswald A, Weymann A, Tsagakis K, Zubarevich A, Thielmann M, Schmack B, Ruhparwar A, Karmonik C. First insights into the role of wall shear stress in the development of a distal stent graft induced new entry through computational fluid dynamics simulations. *J Thorac Dis* 2023;15(2):281-290. doi: 10.21037/jtd-22-1206